

Steric control of the reactivity of moderately hindered tris(pyrazolyl)borates with copper(II) salts †

Li Mei Lindy Chia,^a Sanja Radojevic,^b Ian J. Scowen,^{b,c} Mary McPartlin^b and Malcolm A. Halcrow^{*d}

^a Department of Chemistry, University of Cambridge, Lensfield Road, Cambridge, UK CB2 1EW

^b School of Applied Chemistry, University of North London, 166–220 Holloway Road, London, UK N7 8DB

^c Department of Chemistry and Forensic Sciences, University of Bradford, Bradford, UK BD7 1DP

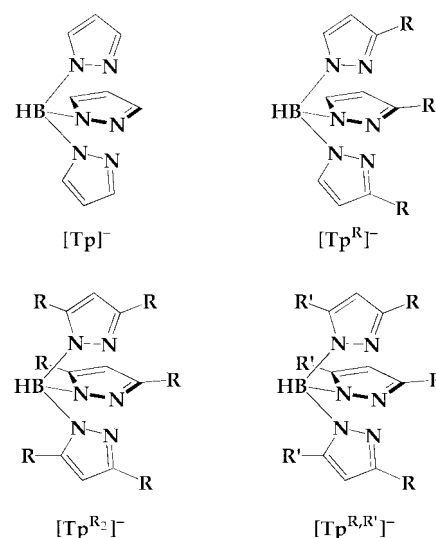
^d School of Chemistry, University of Leeds, Woodhouse Lane, Leeds, UK LS2 9JT.
E-mail: M.A.Halcrow@chem.leeds.ac.uk

Received 8th September 1999, Accepted 19th November 1999

The co-ordination chemistry of the anions tris(3-phenylpyrazolyl)borate ([Tp^{Ph}][−]), tris(3-cyclohexylpyrazolyl)borate ([Tp^{Cy}][−]) and tris(3,5-diphenylpyrazolyl)borate ([Tp^{Ph}][−]) with Cu(O₂CMe)₂·H₂O, CuCl₂ and Cu(BF₄)₂·6H₂O has been investigated. The complex [Cu(O₂CMe)(Tp^{Ph})] (**1**) transforms in solution to the B–N cleavage product [Cu(O₂CMe)(Hpz^{Ph})(Tp^{Ph})] (**2**), whose crystal structure shows two square pyramidal Cu(II) centres in the asymmetric unit, each with a monodentate acetate ligand. The analogous complex [Cu(O₂CMe)(Tp^{Cy})] (**3**) does not undergo this reaction. Reaction of K[Tp^{Cy}] or K[Tp^{Ph}] with one equivalent of CuCl₂ in CH₂Cl₂ yields mixtures of [CuCl(Tp^R)] (R = Cy, Ph₂) and [CuCl(Hpz^R)(Tp^R)] (R = Cy, **5**; R = Ph₂, **6**). Reaction of Cu(BF₄)₂·6H₂O with one equivalent of K[Tp^{Ph}] in CH₂Cl₂ gives [Cu(Hpz^{Ph})₄](BF₄)₂ (**7**) in low yield as the only isolable product. An identical reaction with K[Tp^{Cy}] affords [Cu(Hpz^{Cy})₂(Tp^{Cy})]BF₄ (**8**) in moderate yield. The single crystal structure of **8**·CHCl₃ contains a square pyramidal complex with two N–H···FBF₃ and one Cl₃C–H···FBF₃ hydrogen bonds within each formula unit. Complexation of CuCl₂ by two equivalents of K[Tp^{Ph}] in MeOH affords [Cu(Tp^{Ph})₂] (**9**) in high yield. In contrast, identical reactions employing K[Tp^{Cy}] or K[Tp^{Ph}] yield [Cu(pz^{Cy})(Hpz^{Cy})(Tp^{Cy})] (**10**) or **6** as the major products. The single crystal structure of **10** shows a square pyramidal Cu(II) centre with metric parameters very similar to **8**; although not crystallographically located, the presence of a N–H···N hydrogen bond between the Hpz^{Cy} and [pz^{Cy}][−] ligands can be inferred from the close approach of the pz^{Cy} pyrrolic N atoms. All complexes were characterised by FAB mass spectrometry, microanalysis, IR, UV/vis and EPR spectroscopies.

Introduction

Lewis- or Brønsted-acid induced cleavage of the B–N bonds of tris(pyrazolyl)borates is a well-known feature of their chemistry.^{1,2} We have recently reported an example of this phenomenon, namely the synthesis of [CuX(Hpz^{Ph})(Tp^{Ph})] (X[−] = Cl[−], Br[−]) from equimolar ratios of K[Tp^{Ph}] (Scheme 1) and CuX₂ in CH₂Cl₂.³ This contrasts with similar reactions of other M[Tp^R] (M⁺ = K⁺, Tl⁺) salts with CuCl₂, which afford tetrahedral [CuCl(Tp^R)] when R is very bulky ([Tp^R][−] = [Tp^{Cy}][−],⁴ [Tp^{Bu}][−],⁵ [Tp^{Bu,Me}][−],⁶ [Tp^{Pr}][−];⁷ Scheme 1), or simply [Cu(Tp^R)₂] when R is small ([Tp^R][−] = [Tp][−], [Tp^{Me}][−]; Scheme 1).⁷ The products [CuCl₂(HTp^{Cy})],⁴ [CuCl(dmf)(Tp^{Pr})]⁷ and [{Cu(μ-Cl)(Tp)}₂]⁸ have also been isolated from similar reactions in certain solvents. Hence, the products of such complexations are very dependent on the steric bulk of the tris(pyrazolyl)borate employed. We have recently encountered further examples of this reactivity during our investigations of copper pyrazolylborate chemistry,^{9–12} and present here a comparative study of the products formed by [Tp^{Ph}][−] and the bulkier analogues [Tp^{Cy}][−] and [Tp^{Ph}][−] with Cu(II) salts. Throughout this paper, the Trofimenko system of abbreviations for substituted tris(pyrazolyl)borates¹ is employed (Scheme 1).



Scheme 1 Tris(pyrazolyl)borate nomenclature.

Results and discussion

IR, UV/vis and EPR spectroscopic data for all the complexes in the following discussion are listed in Tables 1 and 2. All UV/vis

† Non-SI unit employed: 1 G = 10^{−4} T.

Table 1 Selected IR and UV/visible spectroscopic data for the complexes in this study

	IR ν/cm^{-1}		UV/vis $\lambda_{\text{max}}/\text{nm}$ ($\epsilon_{\text{max}}/\text{M}^{-1}\text{cm}^{-1}$) CH_2Cl_2
	Nujol	CH_2Cl_2	
$[\text{Cu}(\text{O}_2\text{CMe})(\text{Tp}^{\text{Ph}})]$ (1) ^b	2473, 1514, 1470	2490	247 (sh), 253 (sh), 296 (sh), 735 (78), 975 (sh)
$[\text{Cu}(\text{O}_2\text{CMe})(\text{Hpz}^{\text{Ph}})(\text{Tp}^{\text{Ph}})]$ (2)	2446, 1547, 1494	2490, 2473	244 (46 200), 297 (sh), 370 (sh), 689 (76)
$[\text{Cu}(\text{O}_2\text{CMe})(\text{Tp}^{\text{Cy}})]$ (3)	2480, 1514, 1469	2482	281 (3300), 738 (89), 980 (sh)
$[\text{CuCl}(\text{Hpz}^{\text{Ph}})(\text{Tp}^{\text{Ph}})]$ (4) ^b	3223, 2518	2489, 2472	244 (48 800), 248 (sh), 313 (sh), 708 (103), 925 (sh)
$[\text{CuCl}(\text{Hpz}^{\text{Cy}})(\text{Tp}^{\text{Cy}})]$ (5)	3263, 2469	2482	267 (6300), 290 (sh), 368 (1000), 470 (sh), 715 (104), 940 (sh)
$[\text{CuCl}(\text{Hpz}^{\text{Ph}})(\text{Tp}^{\text{Ph}})]$ (6)	3204, 2600	2618	246 (108 000), 368 (17 200), 430 (sh), 882 (114)
$[\text{Cu}(\text{HPz}^{\text{Ph}})_4](\text{BF}_4)_2$ (7)	3616, 3411, 3317	—	259 (102 500), 352 (15 300), 566 (72), 655 (sh)
$[\text{Cu}(\text{Hpz}^{\text{Cy}})_2(\text{Tp}^{\text{Cy}})]\text{BF}_4$ (8)	3254, 2478	2485	279 (sh), 288 (sh), 330 (880), 612 (52), 730 (sh)
$[\text{Cu}(\text{Tp}^{\text{Ph}})_2]$ (9)	2423	2429	255 (74 500), 320 (sh), 640 (28), 778 (sh)
$[\text{Cu}(\text{Hpz}^{\text{Cy}})(\text{pz}^{\text{Cy}})(\text{Tp}^{\text{Cy}})]$ (10)	2478	2480	265 (3100), 348 (1800), 698 (80), 930 (sh)

^a IR peaks listed correspond to $\nu\{\text{N-H}\}$ (3200–3600 cm^{-1}), $\nu\{\text{B-H}\}$ (2400–2600 cm^{-1}) and $\nu\{\text{O-C-O}\}$ (1400–1600 cm^{-1}). ^b Ref. 3.

Table 2 X-Band EPR data for the complexes in this study (10:1 CH_2Cl_2 -toluene, 293 K and 120 K). Hyperfine and superhyperfine coupling constants are in G

	$\langle g \rangle$	$\langle A \rangle \{^{63,65}\text{Cu}\}$	$\langle A \rangle \{^{14}\text{N}\}$	g_{\parallel}	g_{\perp}	$A_{\parallel} \{^{63,65}\text{Cu}\}$	$A_{\perp} \{^{63,65}\text{Cu}\}$	$A_{\parallel} \{^{14}\text{N}\}$	$A_{\perp} \{^{14}\text{N}\}$
$[\text{Cu}(\text{O}_2\text{CMe})(\text{Tp}^{\text{Ph}})]$ (1) ^a	2.16	44	—	2.29	2.08	148	—	—	—
$[\text{Cu}(\text{O}_2\text{CMe})(\text{Hpz}^{\text{Ph}})(\text{Tp}^{\text{Ph}})]$ (2)	2.15	65	14	2.29	2.06	165	14	13	16
$[\text{Cu}(\text{O}_2\text{CMe})(\text{Tp}^{\text{Cy}})]$ (3)	2.14	42	13	2.30	2.07	148	—	—	—
$[\text{CuCl}(\text{Hpz}^{\text{Ph}})(\text{Tp}^{\text{Ph}})]$ (4) ^a	2.14	62	—	2.26	2.08	163	—	—	—
$[\text{CuCl}(\text{Hpz}^{\text{Cy}})(\text{Tp}^{\text{Cy}})]$ (5)	2.12	58	—	2.28	2.07	157	—	—	—
$[\text{CuCl}(\text{Hpz}^{\text{Ph}})(\text{Tp}^{\text{Ph}})]$ (6)	2.10	—	—	2.29	2.07	146	—	—	—
$[\text{Cu}(\text{Hpz}^{\text{Ph}})_4](\text{BF}_4)_2$ (7)	2.13	80	14	2.26	2.05	180	—	—	—
$[\text{Cu}(\text{Hpz}^{\text{Cy}})_2(\text{Tp}^{\text{Cy}})]\text{BF}_4$ (8)	2.14	70	15	2.27	2.05	171	—	—	—
$[\text{Cu}(\text{Tp}^{\text{Ph}})_2]$ (9)	2.12	41	15	2.28	2.05	144	—	—	—
$[\text{Cu}(\text{pz}^{\text{Cy}})(\text{Hpz}^{\text{Cy}})(\text{Tp}^{\text{Cy}})]$ (10)	2.14	65	15	2.26	2.05	171	—	—	—

^a Ref. 3.

Table 3 Selected bond lengths (\AA) and angles ($^\circ$) at copper in the single crystal X-ray structure of $[\text{Cu}(\text{O}_2\text{CMe})(\text{Hpz}^{\text{Ph}})(\text{Tp}^{\text{Ph}})]$ (**2**)

Molecule 1		Molecule 2	
Cu(1)–N(12)	2.257(4)	Cu(2)–N(62)	2.347(4)
Cu(1)–N(22)	2.020(4)	Cu(2)–N(72)	2.054(4)
Cu(1)–N(32)	2.049(5)	Cu(2)–N(82)	2.013(4)
Cu(1)–N(41)	1.978(4)	Cu(2)–N(91)	1.992(4)
Cu(1)–O(51)	1.957(3)	Cu(2)–O(53)	1.933(3)
N(12)–Cu(1)–N(22)	90.4(2)	N(62)–Cu(2)–N(72)	88.6(2)
N(12)–Cu(1)–N(32)	90.9(2)	N(62)–Cu(2)–N(82)	90.8(2)
N(12)–Cu(1)–N(41)	93.5(2)	N(62)–Cu(2)–N(91)	91.5(2)
N(12)–Cu(1)–O(51)	101.6(2)	N(62)–Cu(2)–O(53)	103.5(2)
N(22)–Cu(1)–N(32)	84.8(2)	N(72)–Cu(2)–N(82)	86.9(2)
N(22)–Cu(1)–N(41)	173.4(2)	N(72)–Cu(2)–N(91)	176.4(2)
N(22)–Cu(1)–O(51)	89.0(2)	N(72)–Cu(2)–O(53)	89.9(2)
N(32)–Cu(1)–N(41)	89.8(2)	N(82)–Cu(2)–N(91)	89.4(2)
N(32)–Cu(1)–O(51)	166.1(2)	N(82)–Cu(2)–O(53)	165.3(2)
N(41)–Cu(1)–O(51)	95.4(2)	N(91)–Cu(2)–O(53)	93.5(2)

and solution IR spectra in the following discussion were run in CH_2Cl_2 at 293 K, while solution EPR spectra were obtained in 10:1 CH_2Cl_2 -toluene at 293 K and 120 K.

Reactions of $\text{K}[\text{Tp}^{\text{R}}]$ with $\text{Cu}(\text{O}_2\text{CMe})_2 \cdot \text{H}_2\text{O}$

As we have previously reported,³ complexation of $\text{Cu}(\text{O}_2\text{CMe})_2 \cdot \text{H}_2\text{O}$ with $\text{K}[\text{Tp}^{\text{Ph}}]$ in CH_2Cl_2 initially affords $[\text{Cu}(\text{O}_2\text{CMe})(\text{Tp}^{\text{Ph}})]$ (**1**), containing a chelating acetate ligand. However, we have since observed that recrystallised samples of **1** often exhibit additional $\nu\{\text{B-H}\}$ and $\nu\{\text{O-C-O}\}$ vibrations by IR, attributable to a contaminant that we could not separate from the bulk material. We suspected that this new species might be a 1:1 cleavage product; in order to confirm this hypothesis, a 1:1:1 mixture of $\text{Cu}(\text{O}_2\text{CMe})_2 \cdot \text{H}_2\text{O}$, $\text{K}[\text{Tp}^{\text{Ph}}]$ and Hpz^{Ph} was reacted in CH_2Cl_2 , cleanly producing a blue-green crystalline compound **2** whose $\nu\{\text{B-H}\}$ and $\nu\{\text{O-C-O}\}$ vibrations were identical to those of the contaminant species

(Table 1). Microanalysis was consistent with the formulation $[\text{Cu}(\text{O}_2\text{CMe})(\text{Hpz}^{\text{Ph}})(\text{Tp}^{\text{Ph}})]$ for **2**. Ambiguously, however, and in contrast to $[\text{CuCl}(\text{Hpz}^{\text{R}})(\text{Tp}^{\text{R}})]$ ($\text{R} = \text{Ph}, \text{Cy}$; see below) no $\nu\{\text{N-H}\}$ vibration was evident by IR spectroscopy. The identity of **2** was therefore confirmed by a single-crystal X-ray structure determination.

The structure of **2** contains two independent molecules per asymmetric unit, both of which exhibit a square pyramidal geometry at copper with tridentate $[\text{Tp}^{\text{Ph}}]^-$ and monodentate Hpz^{Ph} and acetate ligands (Fig. 1, Table 3). The two molecules differ in their apical Cu–N bond lengths, which are $\text{Cu}(1)\text{--N}(12) = 2.257(4)$ and $\text{Cu}(2)\text{--N}(62) = 2.347(4)$ \AA . This difference is reflected in the pitches of the apical $[\text{Tp}^{\text{Ph}}]^-$ phenyl substituents relative to the planes of the pyrazole rings; for molecule 1, the dihedral angle between the planes $[\text{N}(11), \text{N}(12), \text{C}(11)\text{--C}(13)]$ and $[\text{C}(14)\text{--C}(19)]$ is $44.9(2)^\circ$, while for molecule 2 the dihedral angle formed by $[\text{N}(61), \text{N}(62), \text{C}(61)\text{--C}(63)]$ and $[\text{C}(64)\text{--C}(69)]$ is $20.9(2)^\circ$. Other metric parameters within the two molecules show only small differences, however. The structure resembles that previously reported for $[\text{Mn}(\text{O}_2\text{CPh})(\text{Hpz}^{\text{Pr}_3})(\text{Tp}^{\text{Pr}_3})]$,¹³ in that there is an intramolecular hydrogen bond between the Hpz^{Ph} pyrrolic N–H group and the non-coordinated acetate O atom, forming a 7-membered ring system [for molecule 1; $\text{O}(52) \cdots \text{N}(42)$ 2.612(5) \AA , $\text{O}(52) \cdots \text{H}(42\text{N})\text{--N}(42) = 149.0^\circ$; for molecule 2; $\text{O}(54) \cdots \text{N}(92)$ 2.650(5) \AA , $\text{O}(54) \cdots \text{H}(92\text{N})\text{--N}(92)$ 156.3 $^\circ$].

It is instructive to compare the structure of **2** to that we have previously reported for $[\text{CuCl}(\text{Hpz}^{\text{Ph}})(\text{Tp}^{\text{Ph}})]$.³ In the chloro complex, an intramolecular hydrogen bond between the chloro ligand and the Hpz^{Ph} N–H group forms an almost planar 5-membered ring, so that the Hpz^{Ph} pyrazole ring is almost parallel to the basal plane of the complex. This allows the formation of a π -stacking interaction between the Hpz^{Ph} ligand and the apical $[\text{Tp}^{\text{Ph}}]^-$ phenyl substituent, whose steric consequences give rise to a very distorted coordination geometry at Cu. In **2**, the conformation of the 7-membered hydrogen-bonded ring causes the Hpz^{Ph} ligand to tilt substantially away from the basal

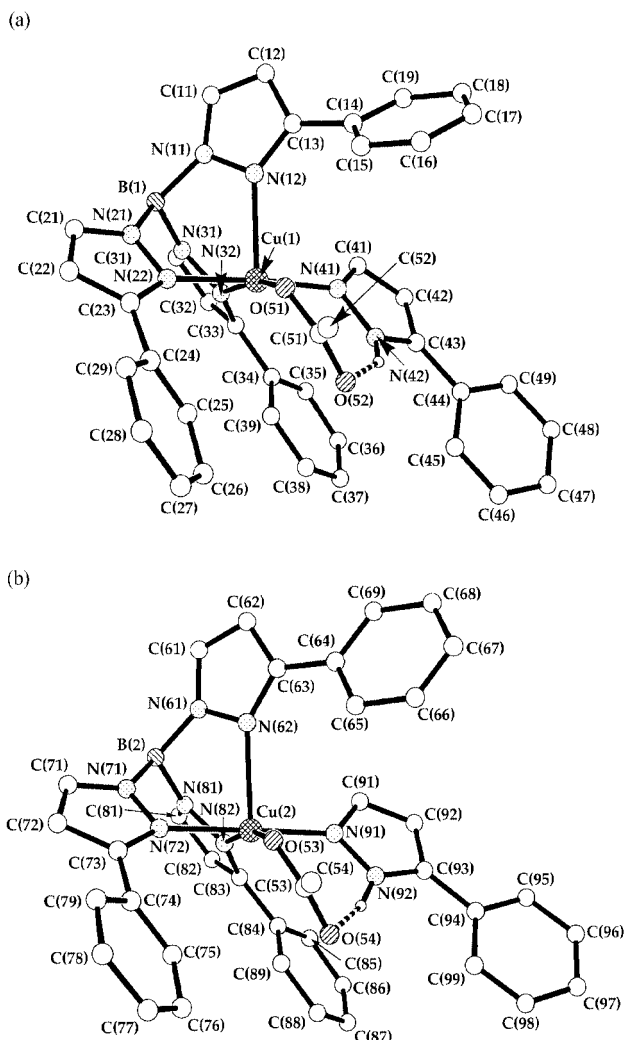


Fig. 1 Structure of the $[\text{Cu}(\text{O}_2\text{CMe})(\text{Hpz}^{\text{Ph}})(\text{Tp}^{\text{Ph}})]$ complex molecules in the crystal of **2**, showing the atom numbering scheme adopted: (a) molecule 1; (b) molecule 2. For clarity, all B- and C-bound H atoms have been omitted.

plane of the complex. Hence, the average dihedral angle between the least squares CuN_4O basal plane and the plane of the Hpz^{Ph} pyrazole ring for the two molecules of **2** is 52.0° , compared to 29.7° in $[\text{CuCl}(\text{Hpz}^{\text{Ph}})(\text{Tp}^{\text{Ph}})]$. As a result, no π -stacking is possible between the $[\text{Tp}^{\text{Ph}}]^-$ phenyl rings and Hpz^{Ph} ligand in **2**, and the Cu(II) centres in this complex have a more regular square pyramidal stereochemistry.

In addition to a d–d absorption at $\lambda_{\text{max}} = 689 \text{ nm}$ ($\epsilon_{\text{max}} = 76 \text{ M}^{-1} \text{ cm}^{-1}$) and $[\text{Tp}^{\text{Ph}}]^-/\text{Hpz}^{\text{Ph}} \pi \rightarrow \pi^*$ band at 244 nm ($46\,200$), the UV/vis spectrum of **2** in CH_2Cl_2 exhibits shoulders at 297 and 370 nm which, from comparison with the spectra of $[\text{CuX}(\text{Hpz}^{\text{Ph}})(\text{Tp}^{\text{Ph}})]$ ($\text{X}^- = \text{Cl}^-, \text{Br}^-$),³ we assign to carboxylate-to-Cu LMCT transitions. Complex **2** exhibits well-resolved X-band spectra (Table 2). In fluid solution **2** shows a 4-line spectrum showing ^{14}N splitting on the $m_I = -3/2$ line, while at 120 K an axial spectrum with well-resolved hyperfine and superhyperfine interactions in the parallel and perpendicular regions was obtained. This spectrum was simulated assuming superhyperfine coupling to 4 ^{14}N nuclei, using the parameters listed in Table 2. The axial nature of the spin system was confirmed by running a Q-band spectrum, which showed identical g and $A_{\parallel}\{^{63,65}\text{Cu}\}$ values to the X-band spectra, but no longer exhibited resolvable couplings in the perpendicular region. The solution visible and EPR spectra of **2** are entirely consistent with its co-ordination geometry in the crystal,^{14,15} and constitute strong evidence that the molecular structure of **2** is retained upon dissolution.

Reaction of $\text{Cu}(\text{O}_2\text{CMe})_2 \cdot \text{H}_2\text{O}$ with $\text{K}[\text{Tp}^{\text{Cy}}]$ in CH_2Cl_2 cleanly affords $[\text{Cu}(\text{O}_2\text{CMe})(\text{Tp}^{\text{Cy}})]$ (**3**), whose IR, UV/vis and EPR spectra closely match **1** and other $[\text{Cu}(\text{O}_2\text{CMe})(\text{Tp}^{\text{R}})]$ species, which all contain chelating acetate ligands.^{3,16} In contrast to **1**, conversion of **3** to $[\text{Cu}(\text{O}_2\text{CMe})(\text{Hpz}^{\text{Cy}})(\text{Tp}^{\text{Cy}})]$ was not detected in recrystallised samples of this compound, or following a 2 h reflux in CHCl_3 . Possibly for steric reasons, $\text{K}[\text{Tp}^{\text{Ph}}]$ does not react with $\text{Cu}(\text{O}_2\text{CMe})_2 \cdot \text{H}_2\text{O}$ in CH_2Cl_2 or MeCN at room temperature or under reflux.

Reactions of $\text{K}[\text{Tp}^{\text{R}}]$ with CuCl_2

Following our synthesis for $[\text{CuCl}(\text{Hpz}^{\text{Ph}})(\text{Tp}^{\text{Ph}})]$ (**4**),³ treatment of CuCl_2 with $\text{K}[\text{Tp}^{\text{Cy}}]$ or $\text{K}[\text{Tp}^{\text{Ph}}]$ in CH_2Cl_2 at room temperature affords dark brown solutions, which in both cases yield brown and green solid products upon layering with hexanes. For both ligands these products had very similar solubilities, so that we were only able to separate them manually. For the $\text{K}[\text{Tp}^{\text{Cy}}]$ reaction the two products were obtained as well-formed crystals in approximately equal proportions. The brown and green species were respectively assigned by microanalysis as the previously reported $[\text{CuCl}(\text{Tp}^{\text{Cy}})]$ ⁴ and the new compound $[\text{CuCl}(\text{Hpz}^{\text{Cy}})(\text{Tp}^{\text{Cy}})]$ (**5**), the latter complex bearing a close resemblance to **4** by IR, UV/vis and EPR spectroscopies (Tables 1 and 2). Complex **5** is the third product to have been isolated from reactions of equimolar ratios of CuCl_2 with $\text{K}[\text{Tp}^{\text{Cy}}]$.⁴ For the reaction employing $\text{K}[\text{Tp}^{\text{Ph}}]$, the brown product (presumably $[\text{CuCl}(\text{Tp}^{\text{Ph}})]$) was only present in small amounts as a powder contaminant on deep green crystals. These crystals slowly desolvate upon drying *in vacuo*, the dried materials giving slightly variable microanalyses that fit for $[\text{CuCl}(\text{Hpz}^{\text{Ph}})(\text{Tp}^{\text{Ph}})] \cdot x\text{CH}_2\text{Cl}_2$ ($6 \cdot x\text{CH}_2\text{Cl}_2$; $x = 0.5\text{--}1$). This formulation was supported by IR spectroscopy, which showed a sharp peak assignable to $\nu\{\text{N--H}\}$ of a Hpz^{Ph} ligand at 3204 cm^{-1} (Table 1); and by FAB mass spectrometry, which demonstrated the presence of $[\text{Tp}^{\text{Ph}}]^-$ and Cl^- ligation to copper.

Interestingly, **6** forms brown solutions in chlorinated solvents whose d–d maximum $[\lambda_{\text{max}} = 882 \text{ nm}$ ($\epsilon_{\text{max}} = 114 \text{ M}^{-1} \text{ cm}^{-1}$) in CH_2Cl_2] is substantially red-shifted compared to **4** and **5** (Table 1) and is suggestive of a tetrahedral Cu(II) centre.¹⁴ This implied to us that **6** might undergo substantial Hpz^{Ph} ligand dissociation in CH_2Cl_2 to yield $[\text{CuCl}(\text{Tp}^{\text{Ph}})]$ as the dominant species in solution. However, the frozen solution EPR spectrum of **6**, which forms a brown glass, shows pseudoaxial symmetry with g values very similar to **4** and **5** and an $A_{\parallel}\{^{63,65}\text{Cu}\}$ constant which is more typical of a tetragonal than a tetrahedral Cu(II) centre¹⁵ (Table 2). A very similar spectrum was obtained from powdered crystals of **6** at 120 K ($g_{\parallel} = 2.28$, $g_{\perp} = 2.08$, $A_{\parallel}\{^{63,65}\text{Cu}\} = 149 \text{ G}$). These EPR spectra differ greatly from those of trigonally distorted tetrahedral $[\text{CuX}(\text{Tp}^{\text{R}})]$ ($\text{X}^- = \text{halide, thiolate, triflate}$) complexes.^{5,7,16} Therefore, **6** is almost certainly a 5-co-ordinate complex analogous to **4** and **5**, which retains its integrity upon dissolution. Presumably the anomalously high-wavelength d–d absorption shown by **6** reflects a more dramatic, sterically induced distortion away from tetragonality than that exhibited by **4**.³

Reactions of $\text{K}[\text{Tp}^{\text{R}}]$ with hydrated $\text{Cu}(\text{BF}_4)_2$

The reaction of $\text{Cu}(\text{BF}_4)_2 \cdot x\text{H}_2\text{O}$ ($x \approx 4$) with 1 molar equivalent of $\text{K}[\text{Tp}^{\text{Ph}}]$ in CH_2Cl_2 at room temperature gives a green solution that yields both oily and solid material upon layering with Et_2O or hexanes. The deep blue–green solid material was separated manually and recrystallised from CH_2Cl_2 –hexanes. This product, which formed in 22% overall yield with respect to the pyrazole content of the $[\text{Tp}^{\text{Ph}}]^-$ employed, was identified as $[\text{Cu}(\text{Hpz}^{\text{Ph}})_4](\text{BF}_4)_2$ (**7**) by comparison with a genuine sample prepared from $\text{Cu}(\text{BF}_4)_2 \cdot x\text{H}_2\text{O}$ and 4 molar equivalents of Hpz^{Ph} . The UV/vis and EPR spectra of this compound (Tables 1 and 2) are comparable to those previously discussed for tetrakis-complexes of $\text{Cu}(\text{BF}_4)_2$ with pyrazole and its methyl-

Table 4 Selected bond lengths (Å) and angles (°) at copper in the single crystal X-ray structure of $[\text{Cu}(\text{Hpz}^{\text{Cy}})_2(\text{Tp}^{\text{Cy}})]\text{BF}_4 \cdot \text{CHCl}_3$ (**8**· CHCl_3). Primed atoms are related to unprimed atoms by the relation $x, -y + \frac{1}{2}, z$

Cu–N(1)	2.260(11)
Cu–N(2)	2.008(7)
Cu–N(3)	2.022(7)
N(1)–Cu–N(2)	90.8(3)
N(1)–Cu–N(3)	93.4(3)
N(2)–Cu–N(2')	85.0(4)
N(2)–Cu–N(3)	89.6(3)
N(2)–Cu–N(3')	173.3(3)
N(3)–Cu–N(3')	95.4(4)

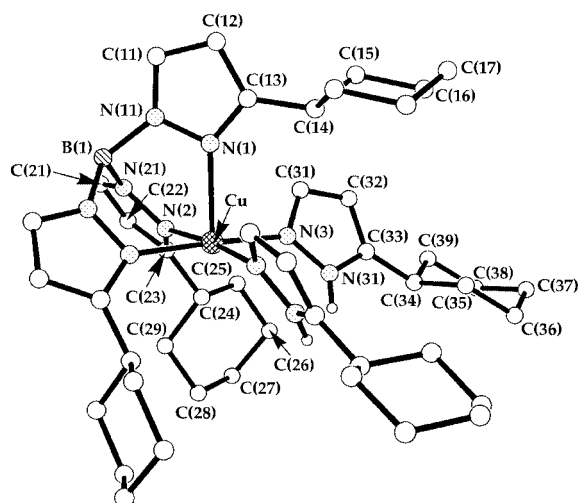


Fig. 2 Structure of the $[\text{Cu}(\text{Hpz}^{\text{Cy}})_2(\text{Tp}^{\text{Cy}})]^+$ complex cation in the crystal of **8**· CHCl_3 , showing the atom numbering scheme adopted. For clarity, all B- and C-bound atoms have been omitted.

ated derivatives, which are presumed to adopt regular square planar geometries.¹⁷ Consistent with this, 8 of the 9 $\langle A\{^{14}\text{N}\} \rangle$ lines expected from coupling to 4 chemically equivalent ^{14}N nuclei can be clearly discerned in the fluid solution EPR spectrum of **7**, while the ratio $g_{\parallel}/A_{\parallel}\{^{63,65}\text{Cu}, \text{cm}^{-1}\}$ is 119 cm (Table 2), within the range expected for a near-planar $\text{Cu}^{\text{II}}\text{N}_4$ centre.¹⁸

In contrast to the above reaction, treatment of $\text{Cu}(\text{BF}_4)_2 \cdot x\text{H}_2\text{O}$ with 1 molar equivalent of $\text{K}[\text{Tp}^{\text{Cy}}]$ in CH_2Cl_2 at room temperature rapidly affords a blue solution, from which a blue crystalline product **8** can be cleanly isolated in 43% yield by filtration, concentration and layering with hexanes. The IR spectrum of this product shows the presence of $[\text{Tp}^{\text{Cy}}]^-$ and BF_4^- , together with a strong $\nu\{\text{N–H}\}$ absorbance that is indicative of Hpz^{Cy} ligation; in addition, the solution EPR spectrum of **8** resembles those of **2**, **4** and **5**, suggesting that **8** contains a square pyramidal $\text{Cu}(\text{II})$ ion. Microanalytical data for **8** could be fit to several potential formulations, however, and **8** was only identified as $[\text{Cu}(\text{Hpz}^{\text{Cy}})_2(\text{Tp}^{\text{Cy}})]\text{BF}_4$ from the single crystal X-ray analysis described below.

Crystals of **8** were grown from CHCl_3 –hexanes. An X-ray structural analysis showed a square pyramidal complex cation, BF_4^- anion and CHCl_3 solvent molecule all lying on sites of crystallographic m symmetry (Fig. 2, Table 4). Because of the crystallographic symmetry, the basal donors N(2), N(3), N(2') and N(3') are perfectly coplanar. The Hpz^{Cy} pyrrolic proton H(31A) is hydrogen-bonded to three F atoms of the disordered BF_4^- anion, with $\text{N} \cdots \text{F}$ distances of 2.87(2)–3.01(2) Å (Fig. 3). The H atom of the CHCl_3 molecule is also hydrogen bonded to F(2), with $\text{C(1)} \cdots \text{F(2)} = 3.05(2)$ Å (Fig. 3).

Reaction of $\text{Cu}(\text{BF}_4)_2 \cdot x\text{H}_2\text{O}$ with 1 molar equivalent of $\text{K}[\text{Tp}^{\text{Ph}}]$ under the above conditions yielded a pale green solution, which deposited copious amounts of Hpz^{Ph} upon layering with hexanes. No copper-containing species could be isolated from this reaction.

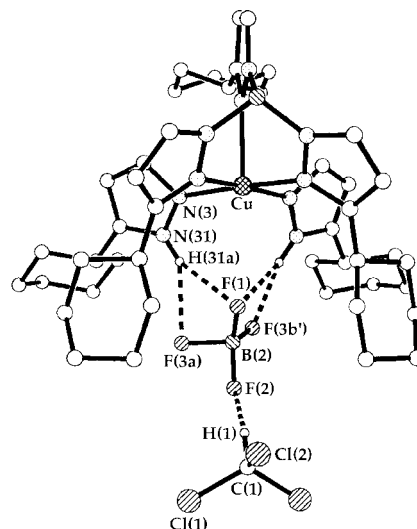


Fig. 3 View of the $[\text{Cu}(\text{Hpz}^{\text{Cy}})_2(\text{Tp}^{\text{Cy}})]\text{BF}_4 \cdot \text{CHCl}_3$ asymmetric unit in the crystal of **8**· CHCl_3 , emphasising the hydrogen bonding within the lattice. One orientation of the disordered BF_4^- anion is shown. Primed atoms are related to unprimed atoms by the relation $x, -y + \frac{1}{2}, z$. For clarity, all H atoms not involved in intermolecular interactions have been omitted.

Reactions of $\text{Cu}(\text{II})$ salts with 2 molar equivalents of $\text{K}[\text{Tp}^{\text{R}}]$

Reaction of CuCl_2 with 2 molar equivalents of $\text{K}[\text{Tp}^{\text{Ph}}]$ in refluxing MeOH affords a mustard precipitate which, although only poorly soluble, could be recrystallised in small amounts from CH_2Cl_2 – MeOH . This solid was formulated as the expected product $[\text{Cu}(\text{Tp}^{\text{Ph}})_2]$ (**9**) by CHN microanalysis, IR spectroscopy, which showed the presence of $[\text{Tp}^{\text{Ph}}]^-$ only, and FAB mass spectrometry. By analogy with other structurally characterised $[\text{M}(\text{Tp}^{\text{Ph}})_2]$ complexes,¹⁹ **9** is proposed to adopt a near-octahedral geometry. Consistent with this proposal, the visible and EPR spectra of **9** (Tables 1 and 2) are similar to those shown by six-co-ordinate $[\text{Cu}(\text{Tp})_2]$.²⁰ Interestingly, however, the IR spectra of **9** and $[\text{M}(\text{Tp}^{\text{Ph}})_2]$ ($\text{M} = \text{Mn}, \text{Fe}^{19}$) are not superimposable, the $\nu\{\text{B–H}\}$ vibration for **9** in the solid state and in solution (Table 1) being *ca.* 50 cm^{-1} lower than for the literature compounds. In the absence of a crystal structure of **9**, the reason for this difference is unclear.

In contrast to the above results, an identical reaction employing 2 molar equivalents of $\text{K}[\text{Tp}^{\text{Cy}}]$ afforded a blue solid product **10** which did not analyse as $[\text{Cu}(\text{Tp}^{\text{Cy}})_2]$ and whose IR spectrum, while still showing the presence of $[\text{Tp}^{\text{Cy}}]^-$, is more complex than that of **9**. The FAB mass spectrum of **10** shows the same fragment ions as that of **8**, while the solution EPR spectrum of **10** also closely resembles that of **8** (Table 2), suggesting that these complexes have near-identical molecular structures. This proposal was confirmed when **10** was identified as $[\text{Cu}(\text{pz}^{\text{Cy}})(\text{Hpz}^{\text{Cy}})(\text{Tp}^{\text{Cy}})]$ from the single crystal X-ray analysis described below. The reason for our obtaining **10** rather than $[\text{Cu}(\text{Hpz}^{\text{Cy}})_2(\text{Tp}^{\text{Cy}})]\text{Cl}$ from this reaction is uncertain, but may reflect the improved basicity of Cl^- compared to the BF_4^- counterion present in **8**. Solutions of CuCl_2 and 2 equivalents of $\text{K}[\text{Tp}^{\text{Ph}}]$ in MeOH at room temperature produce a pale green precipitate of **6**, in improved yields compared to the synthesis described earlier.

Recrystallisation of **10** from CH_2Cl_2 –hexanes afforded a mixture of blue blocks and green needles. Both sets of crystals gave a blue powder when ground up, and afforded identical IR spectra. Hence it was concluded that the two forms contained the same complex compound, presumably differing only in their degree of solvation and/or apical Cu–N distance (*cf.* the structure of **2**, see above). Supporting this idea, the blue form (which is solvent-free by X-ray analysis {see below} but appears to absorb water slowly) analysed consistently as $\text{10} \cdot \text{H}_2\text{O}$ after dry-

Table 5 Selected bond lengths (Å) and angles (°) at copper in the single crystal X-ray structure of [Cu(pz^{Cy})(Hpz^{Cy})(Tp^{Cy})] (**10**)

Cu–N(1)	2.194(8)
Cu–N(2)	2.033(8)
Cu–N(3)	2.055(7)
Cu–N(4)	1.976(7)
Cu–N(5)	2.004(8)
N(1)–Cu–N(2)	91.9(3)
N(1)–Cu–N(3)	89.6(3)
N(1)–Cu–N(4)	97.3(3)
N(1)–Cu–N(5)	97.8(3)
N(2)–Cu–N(3)	83.7(3)
N(2)–Cu–N(4)	91.0(3)
N(2)–Cu–N(5)	169.4(3)
N(3)–Cu–N(4)	171.5(3)
N(3)–Cu–N(5)	91.9(3)
N(4)–Cu–N(5)	92.2(3)

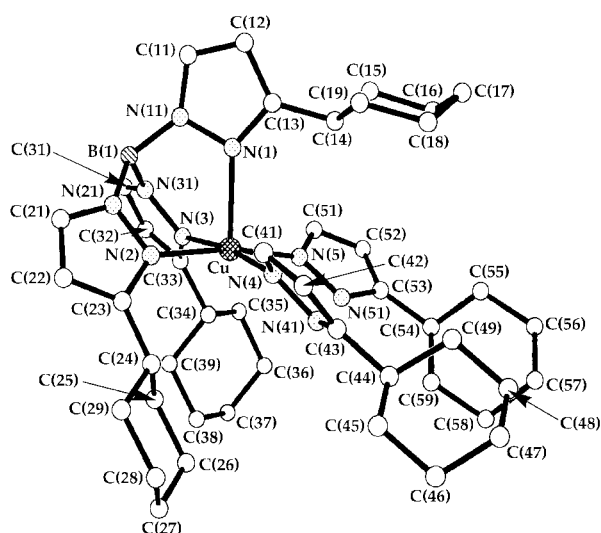


Fig. 4 View of the [Cu(pz^{Cy})(Hpz^{Cy})(Tp^{Cy})] molecule in the crystal of **10**. For clarity, all B- and C-bound H atoms have been omitted. The Hpz^{Cy} N–H proton was not located directly, but is assumed to be involved in hydrogen bonding between N(41) and N(51) [N(41)⋯N(51) = 2.61(1) Å].

ing, while dried samples of the green form analysed approximately as **10**·1/2CH₂Cl₂ (see the Experimental section). Only the blue crystals were therefore structurally analysed. This X-ray structure determination showed one complex molecule per asymmetric unit lying on a general position (Fig. 4, Table 5). The Cu(II) centre lies within a near-regular square-pyramidal geometry, with a rather short ^{3,9–12,21} apical Cu–N(1) distance of 2.194(8) Å. Although this Cu–N bond is shorter in **10** compared to **8**, all other Cu–N distances in **10** and **8** are crystallographically indistinguishable, while corresponding N–Cu–N angles in the two structures differ by <4° (Tables 4 and 5).

The Hpz^{Cy} pyrrolic proton could not be located in the structure of **10**, and is presumably disordered between both pyrazole rings in the molecule. However, its presence can be inferred from charge considerations, and from the following structural comparisons between **8** and **10**. First, the distance between the two pyrazole pyrrolic N atoms in **10** {N(41)⋯N(51) = 2.61(1) Å} is much shorter than the equivalent distance in **8** {N(31)⋯N(31') = 3.67(1) Å}. Second, the dihedral angle between the planes of the two Hpz^{Cy} ligands in **10**, [N(4), N(41), C(41)–C(43)]–[N(5), N(51), C(51)–C(53)] = 135.7(3)°, is more obtuse than the equivalent dihedral angle in **8** {[N(3), N(31), C(31)–C(33)]–[N(3'), N(31'), C(31')–C(33')]} = 114.8(3)°. These differences are both consistent with the presence of a N–H⋯N hydrogen bond between the Hpz^{Cy} and [pz^{Cy}][–] ligands in **10**,

which is not exhibited by **8**. A similar N–H⋯N bonding motif is present in the crystal structure of [{Pt(pz)₂(μ-Hpz)₂}]₂.²²

Concluding remarks

This study has demonstrated that the co-ordination chemistry of Cu(II) salts with hindered tris(pyrazolyl)borates is rather complicated, with a marked tendency towards the formation of B–N cleavage products. This complexity of behaviour has not been noted previously in reactions of [Tp^R][–] with other first row transition ions. In particular, complexation of K[Tp^{Ph}]²³ or other moderately hindered tris(pyrazolyl)borates such as K[Tp^{Pr}]²⁴, K[Tp^{Tn}]²⁵, Ti[Tp^{Mes}]²⁶ or Ti[Tp^{Np}]²⁷ (Tn = thien-2-yl, Mes = mesityl, Np = neopentyl) with ZnX₂, NiX₂ or CoX₂ (X[–] = Cl[–], I[–], N₃[–], NCO[–], NCS[–], MeCO₂[–]) salts cleanly affords the corresponding [MX(Tp^R)], [M(μ-X)(Tp^R)₂] or [MX(solv)(Tp^R)] (solv = thf, dmf) species, depending on X[–] or the steric bulk of 'R', with no pyrazole-containing products having been reported from any of these reactions. In addition, linkage isomerisation to a bis(3-substitutedpyrazolyl)(5-substitutedpyrazolyl)borate, which is a sterically driven process undergone by [Tp^{Pr}][–],²⁴ [Tp^{Mes}][–]²⁶ and [Tp^{Np}][–]²⁷ upon complexation under certain conditions, was not observed from any of our reactions. We ascribe the high reactivity of Cu(II)–[Tp^R][–] complexes towards B–N cleavage to a combination of two factors: the Lewis acidity of the Cu(II) ion, which is greater than for any other divalent first-row transition metal and which will increase the reactivity of a co-ordinated pyrazolylborate; and the unique co-ordinative flexibility of the d⁹ Cu(II) ion, which allows the metal centre to maximise its co-ordination number subject to the steric constraints of the ligand periphery.

Experimental

All manipulations were performed in air using commercial grade solvents. The ligands Hpz^{Ph},²³ K[Tp^{Ph}]^{19,23} K[Tp^{Cy}]⁴ and K[Tp^{Ph}]²⁸ were prepared by the literature procedures. All K[Tp^R] salts employed contained <5% free pyrazole by ¹H NMR. CuCl₂, Cu(O₂CMe)₂·H₂O (Avocado) and Cu(BF₄)₂·xH₂O (x ≈ 4; Aldrich) were used as supplied. Spectroscopic data for all the complexes are given in Tables 1 and 2.

Synthesis of acetato(5-phenylpyrazole)(hydridotris{3-phenylpyrazolyl}borato)copper(II) (**2**)

A mixture of K[Tp^{Ph}] (0.50 g, 1.04 × 10^{–3} mol), Hpz^{Ph} (0.15 g, 1.04 × 10^{–3} mol) and Cu(O₂CMe)₂·H₂O (0.20 g, 1.04 × 10^{–3} mol) was stirred in CH₂Cl₂ (20 cm³) at room temperature for 5 h. The resultant blue–green solution was filtered and reduced to ca. 2 cm³ volume. Addition of a large excess of hexanes and overnight storage at –30 °C yielded analytically pure blue–green crystals. Yield 0.40 g, 72% (found: C, 64.5; H, 4.7; N, 15.6. Calcd. for C₃₈H₃₃BCuN₆O₂: C, 64.5; H, 4.7; N, 15.8%). FAB mass spectrum: *m/z* 711 [⁶³Cu₂(Hpz^{Ph})(H¹¹B{pz^{Ph}})₃]⁺, 648 [⁶³Cu(Hpz^{Ph})(H¹¹B{pz^{Ph}})₃]⁺, 567 [⁶³Cu₂(H¹¹B{pz^{Ph}})₃]⁺, 504 [⁶³Cu(H¹¹B{pz^{Ph}})₃]⁺, 420 [⁶³Cu(O₂CMe)(H¹¹B{pz^{Ph}})₂]⁺, 361 [⁶³Cu(H¹¹B{pz^{Ph}})₂]⁺.

Synthesis of acetato(hydridotris{3-cyclohexylpyrazolyl}borato)copper(II) (**3**)

A mixture of K[Tp^{Cy}] (0.20 g, 0.40 × 10^{–3} mol) and Cu(O₂CMe)₂·H₂O (0.080 g, 0.40 × 10^{–3} mol) was stirred in CH₂Cl₂ (20 cm³) at room temperature for 1 h, yielding a green solution and white precipitate. This was filtered and the filtrate reduced to ca. 2 cm³ volume. Turquoise rods were obtained from this solution upon layering with hexanes. Yield 0.072 g, 31% (found: C, 59.8; H, 7.4; N, 14.4. Calcd. for C₂₉H₄₃BCuN₆O₂: C, 59.8; H, 7.5; N, 14.4%). FAB mass spectrum: *m/z* 585 [⁶³Cu₂(H¹¹B{pz^{Cy}})₃]⁺, 582 [⁶³Cu(H¹¹B{pz^{Cy}})₃](O₂CMe) + H]⁺, 522 [⁶³Cu(H¹¹B{pz^{Cy}})₃]⁺, 432 [⁶³Cu(O₂CMe)(H¹¹B{pz^{Cy}})₂]⁺, 373 [⁶³Cu(H¹¹B{pz^{Cy}})₂]⁺, 213 [⁶³Cu(Hpz^{Cy})]⁺.

Synthesis of chloro(5-cyclohexylpyrazole)(hydridotris{3-phenylpyrazolyl}borato)copper(II) (5)

A solution of $\text{K}[\text{Tp}^{\text{Cy}}]$ (0.20 g, 0.40×10^{-3} mol) and CuCl_2 (0.054 g, 0.40×10^{-3} mol) in CH_2Cl_2 (20 cm^3) was stirred at room temperature for 1 h, yielding a green solution and white precipitate. This was filtered and the filtrate reduced to *ca.* 2 cm^3 volume. Layering this solution with hexanes afforded a mixture of green needles of **5** (yield 0.060 g, 22%) and brown blocks (yield 0.025 g, 11%), which were separated manually. The brown product was identified as the known complex $[\text{CuCl}(\text{Tp}^{\text{Cy}})]^4$ by microanalysis (found: C, 58.0; H, 7.3; N, 14.9. Calcd. for $\text{C}_{27}\text{H}_{40}\text{BClCuN}_{10}$: C, 58.1; H, 7.2; N, 15.1%). Analytical data for **5** (found: C, 60.9; H, 7.7; N, 15.6. Calcd. for $\text{C}_{36}\text{H}_{54}\text{BClCuN}_8$: C, 61.0; H, 7.7; N, 15.8%). FAB mass spectrum: m/z 558 $[\text{Cu}^{35}\text{Cl}(\text{H}^{11}\text{B}\{\text{pz}^{\text{Cy}}\}_3) + \text{H}]^+$, 522 $[\text{Cu}^{35}\text{Cl}(\text{H}^{11}\text{B}\{\text{pz}^{\text{Cy}}\}_3)]^+$, 409 $[\text{Cu}^{35}\text{Cl}(\text{H}^{11}\text{B}\{\text{pz}^{\text{Cy}}\}_2) + \text{H}]^+$, 373 $[\text{Cu}^{35}\text{Cl}(\text{H}^{11}\text{B}\{\text{pz}^{\text{Cy}}\}_2)]^+$, 150 $[\text{Hpz}^{\text{Cy}}]^+$.

Synthesis of chloro(3,5-diphenylpyrazole)(hydridotris{3,5-diphenylpyrazolyl}borato)copper(II) (6)

Method A. $\text{K}[\text{Tp}^{\text{Ph}}]$ (0.50 g, 7.06×10^{-4} mol) and CuCl_2 (0.095 g, 7.06×10^{-4} mol) were stirred in CH_2Cl_2 (50 cm^3) for 1 h, affording a dark brown solution. Filtration, concentration and layering with hexanes afforded dark green crystals which were filtered and washed with hexanes. A brown powder contaminant was removed by suspending the crude solid in hexanes and decanting off the brown suspension. Yield 0.19 g, 37%.

Method B. A mixture of $\text{K}[\text{Tp}^{\text{Ph}}]$ (1.00 g, 1.41×10^{-3} mol) and CuCl_2 (0.095 g, 7.06×10^{-4} mol) in MeOH (50 cm^3) was stirred for 2 h, during which time a pale green precipitate formed which was filtered, washed with cold MeOH and dried *in vacuo*. The green solid became tan upon drying. Recrystallisation from CH_2Cl_2 –hexanes yielded dark green platelets. Yield 0.59 g, 85% (found: C, 70.1; H, 4.7; N, 10.6; Cl, 7.1. Calcd. for $\text{C}_{60}\text{H}_{46}\text{BClCuN}_8 \cdot \text{CH}_2\text{Cl}_2$: C, 70.5; H, 4.5; N, 10.9; Cl, 6.9%). FAB mass spectrum: m/z 952 $[\text{Cu}^{63}(\text{Hpz}^{\text{Ph}})(\text{H}^{11}\text{B}\{\text{pz}^{\text{Ph}}\}_3)]^+$, 830 $[\text{Cu}^{63}(\text{H}^{11}\text{B}\{\text{pz}^{\text{Ph}}\}_3)]^+$, 795 $[\text{Cu}^{63}(\text{H}^{11}\text{B}\{\text{pz}^{\text{Ph}}\}_2)]^+$, 767 $[\text{Cu}^{63}(\text{H}^{11}\text{B}\{\text{pz}^{\text{Ph}}\}_2)]^+$, 732 $[\text{Cu}^{63}(\text{H}^{11}\text{B}\{\text{pz}^{\text{Ph}}\}_2)]^+$, 548 $[\text{Cu}^{63}(\text{H}^{11}\text{B}\{\text{pz}^{\text{Ph}}\}_2)]^+$, 513 $[\text{Cu}^{63}(\text{H}^{11}\text{B}\{\text{pz}^{\text{Ph}}\}_2)]^+$, 283 $[\text{Cu}^{63}(\text{Hpz}^{\text{Ph}})]^+$, 221 $[\text{H}_2\text{pz}^{\text{Ph}}]^+$.

Synthesis of tetrakis(5-phenylpyrazole)copper(II) ditetrafluoroborate (7)

Hpz^{Ph} (0.50 g, 3.47×10^{-3} mol) and $\text{Cu}(\text{BF}_4)_2 \cdot x\text{H}_2\text{O}$ (0.27 g, 8.68×10^{-4} mol) were stirred in CH_2Cl_2 (50 cm^3) at room temperature for 14 h, during which time the solution slowly became dark blue–green. Filtration, concentration and layering of the solution with Et_2O afforded dark blue–green microcrystals, which were filtered, washed with Et_2O and dried *in vacuo*. Yield 0.40 g, 57% (found: C, 53.1; H, 4.1; N, 4.0. Calcd. for $\text{C}_{36}\text{H}_{32}\text{B}_2\text{CuF}_8\text{N}_8$: C, 53.1; H, 4.0; N, 13.8%). FAB mass spectrum: m/z 351 $[\text{Cu}^{63}(\text{Hpz}^{\text{Ph}})_2]^+$, 207 $[\text{Cu}^{63}(\text{Hpz}^{\text{Ph}})]^+$, 145 $[\text{H}_2\text{pz}^{\text{Ph}}]^+$.

Synthesis of bis(5-cyclohexylpyrazole)(hydridotris{3-cyclohexylpyrazolyl}borato)copper(II) tetrafluoroborate (8)

$\text{K}[\text{Tp}^{\text{Cy}}]$ (0.50 g, 1.00×10^{-3} mol) and $\text{Cu}(\text{BF}_4)_2 \cdot x\text{H}_2\text{O}$ (0.24 g, 1.00×10^{-3} mol) were stirred in CH_2Cl_2 (50 cm^3) at room temperature for 1 h, yielding a dark blue solution and white precipitate. Filtration, concentration and layering of the solution with hexanes at -20°C yielded a blue solid, which gave blue crystals from CHCl_3 –hexanes. Yield 0.24 g, 26% (found: C, 56.7; H, 7.2; N, 14.2. Calcd. for $\text{C}_{45}\text{H}_{68}\text{B}_2\text{CuF}_4\text{N}_{10} \cdot 0.5\text{CHCl}_3$: C, 56.3; H, 7.1; N, 14.4%). FAB mass spectrum: m/z 672 $[\text{Cu}^{63}(\text{Hpz}^{\text{Cy}})(\text{H}^{11}\text{B}\{\text{pz}^{\text{Cy}}\}_3)]^+$, 585 $[\text{Cu}^{63}(\text{H}^{11}\text{B}\{\text{pz}^{\text{Cy}}\}_3)]^+$, 523 $[\text{Cu}^{63}(\text{H}^{11}\text{B}\{\text{pz}^{\text{Cy}}\}_3)]^+$, 373 $[\text{Cu}^{63}(\text{H}^{11}\text{B}\{\text{pz}^{\text{Cy}}\}_2)]^+$, 213 $[\text{Cu}^{63}(\text{Hpz}^{\text{Cy}})]^+$.

Synthesis of bis(hydridotris{3-phenylpyrazolyl}borato)copper(II) (9)

$\text{K}[\text{Tp}^{\text{Ph}}]$ (0.50 g, 1.04×10^{-3} mol) and CuCl_2 (0.070 g, 5.20×10^{-4} mol) were stirred in MeOH (50 cm^3) at room temperature for 2 h, affording a mustard-coloured precipitate which was filtered, washed with MeOH and Et_2O , and dried *in vacuo*. The sparingly soluble product formed yellow–green microcrystals from CH_2Cl_2 –MeOH. Yield 0.39 g, 79% (found: C, 63.9; H, 4.5; N, 16.3. Calcd. for $\text{C}_{54}\text{H}_{44}\text{B}_2\text{CuN}_{12} \cdot \text{CH}_2\text{Cl}_2$: C, 64.1; H, 4.5; N, 16.3%). FAB mass spectrum: m/z 802 $[\text{Cu}^{63}(\text{H}^{11}\text{B}\{\text{pz}^{\text{Ph}}\}_3)(\text{H}^{11}\text{B}\{\text{pz}^{\text{Ph}}\}_2)]^+$, 711 $[\text{Cu}^{63}(\text{H}^{11}\text{B}\{\text{pz}^{\text{Ph}}\}_3)(\text{H}^{11}\text{B}\{\text{pz}^{\text{Ph}}\}_2)]^+$, 659 $[\text{Cu}^{63}(\text{H}^{11}\text{B}\{\text{pz}^{\text{Ph}}\}_3)(\text{H}^{11}\text{B}\{\text{pz}^{\text{Ph}}\}_2)]^+$, 648 $[\text{Cu}^{63}(\text{H}^{11}\text{B}\{\text{pz}^{\text{Ph}}\}_3)(\text{H}^{11}\text{B}\{\text{pz}^{\text{Ph}}\}_2)]^+$, 567 $[\text{Cu}^{63}(\text{H}^{11}\text{B}\{\text{pz}^{\text{Ph}}\}_3)]^+$, 504 $[\text{Cu}^{63}(\text{H}^{11}\text{B}\{\text{pz}^{\text{Ph}}\}_3)]^+$, 361 $[\text{Cu}^{63}(\text{H}^{11}\text{B}\{\text{pz}^{\text{Ph}}\}_2)]^+$.

Synthesis of (5-cyclohexylpyrazolide)(5-cyclohexylpyrazole)-(hydridotris{3-cyclohexylpyrazolyl}borato)copper(II) (10)

Method as for **8**, using CuCl_2 (0.07 g, 5.00×10^{-4} mol). The product formed a mixture of blue and green crystals from CH_2Cl_2 –hexanes, which were separated by inspection. Both forms afforded identical IR spectra upon drying. Yield 0.21 g, 42% (Blue form, found: C, 64.2; H, 8.2; N, 16.4. Calcd. for $\text{C}_{45}\text{H}_{67}\text{BCuN}_{10} \cdot \text{H}_2\text{O}$: C, 64.3; H, 8.3; N, 16.7%. Green form, found: C, 63.7; H, 7.9; N, 16.4. Calcd. for $\text{C}_{45}\text{H}_{67}\text{BCuN}_{10} \cdot 0.5\text{CH}_2\text{Cl}_2$: C, 63.2; H, 7.9; N, 16.2%). FAB mass spectrum: m/z 734 $[\text{Cu}^{63}(\text{pz}^{\text{Cy}})(\text{H}^{11}\text{B}\{\text{pz}^{\text{Cy}}\}_3)]^+$, 672 $[\text{Cu}^{63}(\text{Hpz}^{\text{Cy}})(\text{H}^{11}\text{B}\{\text{pz}^{\text{Cy}}\}_3)]^+$, 585 $[\text{Cu}^{63}(\text{H}^{11}\text{B}\{\text{pz}^{\text{Cy}}\}_3)]^+$, 523 $[\text{Cu}^{63}(\text{H}^{11}\text{B}\{\text{pz}^{\text{Cy}}\}_3)]^+$, 373 $[\text{Cu}^{63}(\text{H}^{11}\text{B}\{\text{pz}^{\text{Cy}}\}_2)]^+$, 213 $[\text{Cu}^{63}(\text{Hpz}^{\text{Cy}})]^+$.

Single crystal X-ray structure determinations

Crystals of **2**, **8** and **10** were respectively obtained from toluene, CHCl_3 and CH_2Cl_2 by layering a solution of the complex in the appropriate solvent with hexanes. Experimental details from the structure determinations are given in Table 6. All structures were solved by direct methods (SHELXTL Plus)²⁹ and refined by full matrix least-squares on F^2 (SHELXL93³⁰ or SHELXL97³¹).

CCDC reference number 186/1746.

See <http://www.rsc.org/suppdata/dt/a9/a907258f/> for crystallographic files in .cif format.

X-Ray structure determination of $[\text{Cu}(\text{O}_2\text{CMe})(\text{Hpz}^{\text{Ph}})(\text{Tp}^{\text{Ph}})]$ (2). The structure contained two complex molecules per asymmetric unit. All non-H atoms were refined anisotropically, while all C- and B-bound H atoms were placed in calculated positions. The pyrazole pyrrolic H atoms H(42N) and H(92N) were located in a Fourier difference map ($\theta < 20^\circ$), and their parameters included in the refinement with a refined common U_{iso} of 0.099 \AA^2 .

X-Ray structure determination of $[\text{Cu}(\text{Hpz}^{\text{Cy}})_2(\text{Tp}^{\text{Cy}})]\text{BF}_4 \cdot \text{CHCl}_3$ (8·CHCl₃). The atoms Cu, N(1), N(11), C(11), C(12), C(13), C(14), C(17), B(1), B(2), F(1), F(2), C(1) and Cl(2) lie on sites of crystallographic *m* symmetry. There is disorder of the BF_4^- anion across a crystallographic mirror plane, involving a slight rotation about the B(2)–F(1) bond. One F atom was resolved into two equally occupied components F(3a) and F(3b). Although high isotropic thermal parameters indicated that F(2) is also affected, its location on the mirror plane made resolution impossible. The C–C distances within the cyclohexyl substituents of the complex were constrained to be equal within an e.s.d. of 0.03 \AA , and all H atoms were included in idealised positions.

X-Ray structure determination of $[\text{Cu}(\text{pz}^{\text{Cy}})(\text{Hpz}^{\text{Cy}})(\text{Tp}^{\text{Cy}})]$ (10). No disorder was detected in this structure. The C–C distances within the cyclohexyl substituents of the complex were constrained to be equal within an e.s.d. of 0.03 \AA , and all H atoms were included in idealised positions.

Table 6 Experimental details for the single crystal structure determinations in this study

	[Cu(O ₂ CMe)(Hpz ^{Ph})(Tp ^{Ph})] (2)	[Cu(Hpz ^{Cy}) ₂ (Tp ^{Cy})]BF ₄ ·CHCl ₃ (8 ·CHCl ₃)	[Cu(pz ^{Cy})(Hpz ^{Cy})(Tp ^{Cy})] (10)
Formula	C ₃₈ H ₃₃ BCuN ₈ O ₂	C ₄₆ H ₆₉ B ₂ Cl ₃ CuF ₄ N ₁₀	C ₄₅ H ₆₇ BCuN ₁₀
<i>M_r</i>	708.07	1029.62	821.43
Crystal class	Triclinic	Monoclinic	Monoclinic
Space group	<i>P</i> $\bar{1}$	<i>P</i> 2 ₁ / <i>m</i>	<i>P</i> 2 ₁ / <i>n</i>
<i>a</i> /Å	11.585(2)	11.514(2)	11.410(2)
<i>b</i> /Å	16.787(4)	18.291(3)	21.315(4)
<i>c</i> /Å	18.492(3)	12.439(2)	18.692(4)
<i>a</i> /°	95.11(2)	—	—
<i>β</i> /°	106.08(1)	93.67(1)	95.44(2)
<i>γ</i> /°	94.17(3)	—	—
<i>U</i> /Å ³	3423.8(11)	2614.3(8)	4525(1)
<i>Z</i>	4	2	4
<i>μ</i> (Mo-Kα)/mm ^{−1}	0.685	0.627	0.525
<i>T</i> /K	223(2)	223(2)	223(2)
Measured reflections	13981	3749	7882
Independent reflections	12026	2930	6306
<i>R</i> _{int}	0.039	0.057	0.054
<i>R</i> (<i>F</i>) (<i>I</i> > 2σ <i>I</i>)	0.054	0.072	0.073
<i>wR</i> (<i>F</i> ²)	0.157	0.254	0.265
<i>S</i>	0.980	1.016	0.922

$R = \sum [|F_o| - |F_c|]/\sum |F_o|$, $wR = [\sum w(F_o^2 - F_c^2)/\sum wF_o^4]^{1/2}$.

Other measurements

Infrared spectra were obtained as Nujol mulls pressed between KBr windows, or in NaCl solution cells, between 400 and 4000 cm^{−1} using a Perkin-Elmer Paragon 1000 spectrophotometer. UV/visible spectra were obtained with a Perkin-Elmer Lambda 12 spectrophotometer operating between 200 and 1100 nm, in 1 cm quartz cells. Positive ion fast atom bombardment mass spectra were performed on a Kratos MS890 spectrometer employing a 3-NOBA matrix. CHN microanalyses were performed by the University of Cambridge Department of Chemistry microanalytical service. EPR spectra for **2** were obtained using a Bruker ESP300E spectrometer, fitted with the following attachments: at X-band, an ER4102ST resonator and ER4111VT cryostat; and at Q-band, an ER5106QT resonator and ER4118VT cryostat. Spectral simulations were performed using in-house software which has been described elsewhere.³² X-Band EPR spectra of the other complexes were obtained using a Bruker ER200D spectrometer.

Acknowledgements

The authors acknowledge the Royal Society (London) for a University Research Fellowship to M. A. H., the government of Singapore (L. M. L. C.), the EPSRC (S. R., I. J. S.), the University of Cambridge and the University of Leeds for financial support. We also wish to thank Dr Eric McInnes and Dr Frank Mabbs of the EPSRC CW EPR Service, in the Department of Chemistry of the University of Manchester, for the EPR spectra of **2**.

References

- S. Trofimenko, *Prog. Inorg. Chem.*, 1986, **34**, 115; S. Trofimenko, *Chem. Rev.*, 1993, **93**, 943; N. Kitajima and W. B. Tolman, *Prog. Inorg. Chem.*, 1995, **43**, 419; G. Parkin, *Adv. Inorg. Chem.*, 1995, **42**, 291.
- See e. g. L. G. Hubert-Pfalzgraf and M. Tsunoda, *Polyhedron*, 1983, **2**, 203; D. C. Bradley, M. B. Hursthouse, J. Newton and N. P. C. Walker, *J. Chem. Soc., Chem. Commun.*, 1984, 188; F. A. Cotton, Z. Dori, R. Llusar and W. Schwotzer, *Inorg. Chem.*, 1986, **25**, 3529; G. Backes-Dahmann and J. H. Enemark, *Inorg. Chem.*, 1987, **26**, 3960; D. L. Hughes, G. J. Leigh and D. G. Walker, *J. Chem. Soc., Dalton Trans.*, 1988, 1153; E. Kime-Hunt, K. Spartalian, M. DeRusha, C. M. Nunn and C. J. Carrano, *Inorg. Chem.*, 1989, **28**, 4392; M. M. Taqui Kahn, P. S. Roy, K. Venkatasubramanian and N. H. Kahn, *Inorg. Chim. Acta*, 1990, **176**, 49; R. Alsasser and H. Vahrenkamp, *Chem. Ber.*, 1993, **126**, 695; D. Collison, D. R. Eardley, F. E. Mabbs, A. K. Powell and S. S. Turner, *Inorg. Chem.*, 1993, **32**, 664; F. A. Jalón, A. Otero and A. Rodríguez, *J. Chem. Soc., Dalton Trans.*, 1995, 1629; M. D. Ward, J. S. Fleming, E. Psillakis, J. C. Jeffrey and J. A. McCleverty, *Acta Crystallogr., Sect. C*, 1998, **54**, 609.
- M. A. Halcrow, J. E. Davies and P. R. Raithby, *Polyhedron*, 1997, **16**, 1535.
- A. L. Rheingold, B. S. Haggerty and S. Trofimenko, *Angew. Chem., Int. Ed. Engl.*, 1994, **33**, 1983.
- R. Han, A. Looney, K. McNeill, G. Parkin, A. L. Rheingold and B. S. Haggerty, *J. Inorg. Biochem.*, 1993, **49**, 105; C. E. Ruggiero, S. M. Carrier, W. E. Antholine, J. W. Whittaker, C. J. Cramer and W. B. Tolman, *J. Am. Chem. Soc.*, 1993, **115**, 11285.
- K. Yoon and G. Parkin, *Polyhedron*, 1995, **14**, 811.
- N. Kitajima, K. Fujisawa and Y. Moro-oka, *J. Am. Chem. Soc.*, 1990, **112**, 3210.
- S. G. N. Roundhill, D. M. Roundhill, D. R. Bloomquist, C. Landee, R. D. Willett, D. M. Dooley and H. B. Gray, *Inorg. Chem.*, 1979, **18**, 831.
- M. A. Halcrow, E. J. L. McInnes, F. E. Mabbs, I. J. Scowen, M. McPartlin, H. R. Powell and J. E. Davies, *J. Chem. Soc., Dalton Trans.*, 1997, 4025.
- M. A. Halcrow, L. M. L. Chia, X. Liu, E. J. L. McInnes, L. J. Yellowlees, F. E. Mabbs and J. E. Davies, *Chem. Commun.*, 1998, 2465.
- M. A. Halcrow, L. M. L. Chia, X. Liu, E. J. L. McInnes, L. J. Yellowlees, F. E. Mabbs, I. J. Scowen, M. McPartlin and J. E. Davies, *J. Chem. Soc., Dalton Trans.*, 1999, 1753.
- X. Liu, L. M. L. Chia, S. Radojevic, L. J. Yellowlees, M. McPartlin and M. A. Halcrow, unpublished work.
- N. Kitajima, M. Osawa, N. Tamura, Y. Moro-oka, T. Hirano, M. Hirobe and T. Nagano, *Inorg. Chem.*, 1993, **32**, 1879.
- A. B. P. Lever, *Inorganic Electronic Spectroscopy*, 2nd edn., Elsevier, Amsterdam, 1984, pp. 554–572.
- B. A. Goodman and J. B. Raynor, *Adv. Inorg. Chem.*, 1970, **13**, 135.
- N. Kitajima, K. Fujisawa and Y. Moro-oka, *Inorg. Chem.*, 1990, **29**, 357; W. B. Tolman, *Inorg. Chem.*, 1991, **30**, 4877; N. Kitajima, K. Fujisawa, M. Tanaka and Y. Moro-oka, *J. Am. Chem. Soc.*, 1992, **114**, 9232; D. D. LeCloux, M. C. Keyes, M. Osawa, V. Reynolds and W. B. Tolman, *Inorg. Chem.*, 1994, **33**, 6361.
- J. Reedijk, *Recl. Trav. Chim. Pays-Bas*, 1969, **88**, 1451; J. Reedijk, *Recl. Trav. Chim. Pays-Bas*, 1970, **89**, 605; J. Reedijk, J. C. A. Windhorst, N. H. M. van Ham and W. L. Groeneveld, *Recl. Trav. Chim. Pays-Bas*, 1971, **90**, 234.
- J. Gouteron, S. Jeannin, Y. Jeannin, J. Livage and C. Sanchez, *Inorg. Chem.*, 1984, **23**, 3387.
- D. M. Eichhorn and W. H. Armstrong, *Inorg. Chem.*, 1990, **29**, 3607.
- A. Murphy, B. J. Hathaway and T. J. King, *J. Chem. Soc., Dalton Trans.*, 1979, 1646.
- J. Perkinson, S. Brodie, K. Yoon, K. Mosny, P. J. Carroll, T. V. Morgan and S. J. Nieter Burgmayer, *Inorg. Chem.*, 1991, **30**, 719.
- W. Burger and J. Strähle, *Z. Anorg. Allg. Chem.*, 1986, **539**, 27.

- 23 S. Trofimenko, J. C. Calabrese and J. S. Thompson, *Inorg. Chem.*, 1987, **26**, 1507.
- 24 S. Trofimenko, J. C. Calabrese, P. J. Domaille and J. S. Thompson, *Inorg. Chem.*, 1989, **28**, 1091; S. Trofimenko, J. C. Calabrese, J. K. Kochi, S. Wolowicz, F. B. Hulsbergen and J. Reedijk, *Inorg. Chem.*, 1992, **31**, 3493.
- 25 J. C. Calabrese, P. J. Domaille, S. Trofimenko and G. J. Long, *Inorg. Chem.*, 1991, **30**, 2795.
- 26 A. L. Rheingold, C. B. White and S. Trofimenko, *Inorg. Chem.*, 1993, **32**, 3471.
- 27 J. C. Calabrese and S. Trofimenko, *Inorg. Chem.*, 1992, **31**, 4810.
- 28 N. Kitajima, K. Fujisawa, C. Fujimoto, Y. Moro-oka, S. Hashimoto, T. Kitagawa, K. Toriumi, K. Tatsumi and A. Nakamura, *J. Am. Chem. Soc.*, 1992, **114**, 1277.
- 29 G. M. Sheldrick, SHELXTL Plus, PC version, Siemens Analytical Instruments Inc., Madison WI, 1990.
- 30 G. M. Sheldrick, SHELXL 93, University of Göttingen, 1993.
- 31 G. M. Sheldrick, SHELXL 97, University of Göttingen, 1997.
- 32 F. E. Mabbs and D. Collison, *Electron Paramagnetic Resonance of d Transition Metal Compounds*, Elsevier, Amsterdam, 1992, ch. 7.

Paper a907258f